Received: 15 May 2020 | Revised: 3 August 2020 | Accepted: 4 August 2020

DOI: 10.1002/pro.3926

ARTICLE

THE PROTEIN SOCIETY WILEY

Crystal structure of the nucleotide-metabolizing enzyme NTPDase4

Alexei Gorelik | **Jonathan M. Labriola** | **Katalin Illes** | **Bhushan Nagar**

Department of Biochemistry, McGill University, Montreal, Quebec, Canada

Correspondence
Bhushan Nagar, Department of Biochemistry, McGill University, Room 464, 3649 Promenade Sir-William-Osler, Montreal, QC H3G 0B1, Canada.
Email: bhushan.nagar@mcgill.ca

Funding information
Canadian Institutes of Health Research, Grant/Award Number: MOP-133535

Abstract

The ecto-nucleoside triphosphate diphosphohydrolases (NTPDases) are a family of enzymes found on the cell surface and in the lumen of certain organelles, that are major regulators of purinergic signaling. Their intracellular roles, however, have not been clearly defined. NTPDase4 (UDPase, ENTPD4) is a Golgi protein potentially involved in nucleotide recycling as part of protein glycosylation, and is also found in lysosomes, where its purpose is unknown. To further our understanding of NTPDase4 function, we determined its crystal structure. The enzyme adopts a wide open, inactive conformation. Differences in the nucleotide-binding site relative to its homologs could account for its substrate selectivity. The putative membrane-interacting loop of cell-surface NTPDases is drastically altered in NTPDase4, potentially affecting its inter-domain dynamics at the Golgi membrane.

KEYWORDS

ENTPD4, NTPDase4, nucleotide metabolism, UDPase, X-ray crystallography

1 | INTRODUCTION

Intracellular nucleotides are the building blocks of nucleic acids and serve as energy currency. Outside of the cell, certain released nucleotides including ATP, ADP, UTP, and UDP serve as signaling molecules and activate specific cell surface receptors.[1] Termination of purinergic signaling requires hydrolysis of these molecules, which is carried out by a few enzyme families, including the ecto-nucleoside triphosphate diphosphohydrolases (NTPDases).[2] As these proteins participate in the regulation of crucial physiological processes, including immunity, NTPDase inhibitors are being developed for therapeutic purposes.[3] To this end, it is important to understand the functional and structural differences between members of this family, to allow their selective targeting.

The mammalian NTPDases convert NTPs and NDPs into NMPs, and consist of eight enzymes classified into two groups. NTPDase1, 2, 3, and 8 are double-pass transmembrane proteins found on the cell surface, whereas NTPDase4, 5, 6, and 7 are located on intracellular membranes; soluble forms of NTPDase5 and 6 also exist.[1] The four cell surface homologs are the major nucleotide-hydrolyzing enzymes involved in purinergic signaling.[4] On the other hand, the functions of intracellular NTPDases are less clearly defined; rather than modulating signaling, they are possibly involved in protein synthesis.[1] Protein folding and quality control in the ER, as well as glycosylation reactions in the Golgi, utilize nucleotide-sugars as substrates, resulting in NDPs (mainly UDP and GDP) as byproducts.[5] These NDPs are converted to NMPs for export back to the cytosol. Such a role was proposed for ER NTPDase5[6] and Golgi NTPDase6,[7,8] which share 48% sequence identity, as well as for Golgi NTPDase4,[9] which is 67% identical to NTPDase7 of unknown function. Whereas NTPDase1 and 2 have been structurally characterized,[10–13] structural information is lacking for the intracellular homologs.

Alexei Gorelik and Jonathan M. Labriola are co-authors.

NTPDase4 (UDPase, *ENTPD4*), which was cloned over 20 years ago, is expressed in all tissues.[14] Two isoforms with different intracellular localization patterns were discovered.[9,15] A long isoform of higher abundance is found in lysosomes and autophagic vacuoles,[15] where its function is unknown. A short isoform missing an 8-amino-acid segment localizes to the Golgi.[9] Interestingly, the variants display different metal ion dependencies[14,16] and substrate preferences in terms of nucleobase type and number of phosphates.[9,14,16] Notably, as opposed to the cell surface NTPDases, neither NTPDase4 isoform is active against ATP or ADP. This enzyme may play a role in development of gastric cancer.[17]

In order to improve our understanding of NTPDase4 function, we determined its crystal structure. The protein adopted a wide open, inactive conformation. Comparison of its substrate-binding site with that of its homologs provides clues on the determinants of its substrate selectivity, and will facilitate the development of subtype-specific inhibitors for the NTPDase family.

2 | RESULTS AND DISCUSSION

2.1 | The catalytic domain is composed of two lobes separated by a cleft

NTPDase4 is a transmembrane protein located on the luminal side of the Golgi,[9] lysosomes, and autophagic vacuoles.[15] The enzyme is anchored via an N-terminal and a C-terminal transmembrane helix, with short cytoplasmic segments at both ends (Figure 1a). We determined the crystal structure of the human NTPDase4 luminal portion produced recombinantly in insect cells. This construct is catalytically active (Figure 1c). The protein comprises two lobes, termed domains I and II, that together form the catalytic domain. The lobes are structurally related, each consisting of a central five-stranded mixed β sheet flanked on one side by two or more helices, and on the other side by a single helix (Figure 1b). The lobes are facing each other such that the two single helices are in contact, leaving a wide cleft in the middle of the protein. Domain I is mainly N-terminal, but also includes a helix and a linker immediately preceding the C-terminal transmembrane segment. Domain II is slightly larger, bearing an additional three-stranded β sheet on its periphery. In the crystal structure, both termini are located on the same side of the protein, with linkers of 10 to 16 residues that are disordered (or artificially ordered by crystal contacts) extending toward the two membrane-spanning helices in the native protein.

The enzyme harbors two N-linked glycosylation sites; complete or partial electron density indicates the presence of a glycan on both Asn404 and Asn407 (Figure 1b). Two disulfide bridges stabilize domain II (residues 368–395 and 461–490). In domain I, Cys95 and Cys178 are located on adjacent β strands and are properly oriented for disulfide bond formation (Figure 2c). However, the two side chains are not connected in the crystal

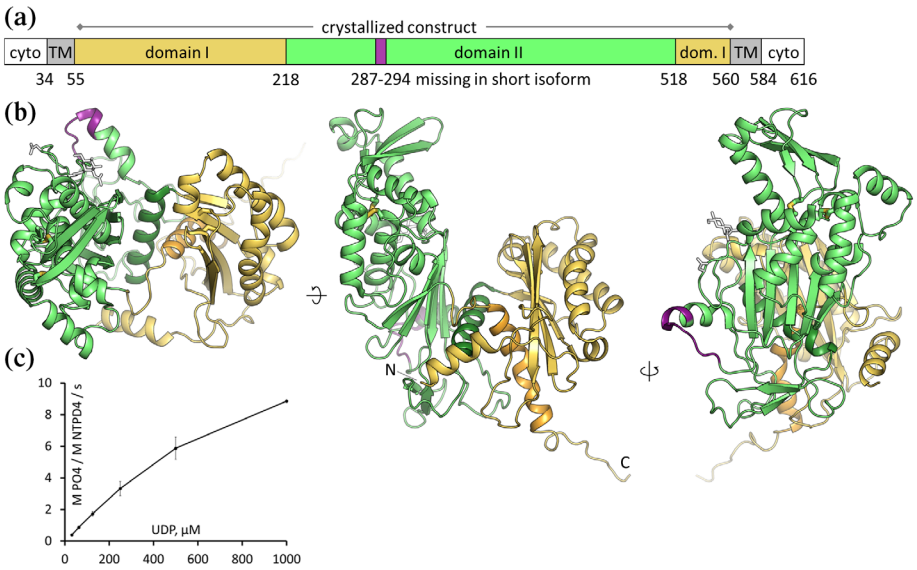

FIGURE 1 Structure of NTPDase4. (a) Domain organization of NTPDase4. The enzyme is composed of a large luminal region flanked by a transmembrane helix (TM) and short cytoplasmic segment (cyto) both at the N- and C-terminus. (b) Crystal structure of the NTPDase4 luminal region, long isoform. The termini are labeled. Number of additional residues between the visible ends and the start of the TM helices: 9 (N) and 4 (C). Disulfide bonds are shown as thick sticks, and the N-linked glycan as well as glycosylated asparagine residues, as white sticks. (c) in vitro UDP hydrolysis by the purified and crystallized construct. Data are the averages and standard deviations of one representative of two experiments, each performed in triplicates

structure, possibly due to a high sensitivity of this linkage to X-ray radiation damage.

2.2 | NTPDase4 adopts an open conformation

The bilobal fold of NTPDase4 is characteristic of the ASKHA structural superfamily of phosphotransferases,[18] and is conserved in the NTPDase family (Pfam: PF01150). Crystal structures of mammalian NTPDase1[10] and NTPDase2[11–13] as well as of homologs from plants[19] and microorganisms[11,20–25] revealed interdomain rotations in these proteins.[10,11] Indeed, formation of a productive enzyme-substrate complex requires a closing motion that brings elements from both domains together.[11] Apo NTPDase4 adopts a more open conformation relative to all other reported NTPDase structures, including other apo ones (Figure 2), resulting in a wider interdomain cleft. This configuration may be influenced by interprotein contacts within the crystal and does not necessarily reflect the range of motion of the native membrane-anchored protein. However, as detailed below, the current conformation is not conducive to proper substrate binding.

NTPDases hydrolyze the terminal phosphate of nucleotide triphosphates (NTPs) or diphosphates (NDPs). Their substrate-binding site, located in the interdomain cleft, can be divided into two sections: the catalytic site and the nucleoside-binding region. The catalytic site contains highly conserved residues that stabilize the two terminal phosphate groups of the substrate (β and γ of NTPs, or α and β of NDPs) as well as a calcium or magnesium ion and its coordinated water molecules.[13] On the other hand, the nucleoside-binding region is more variable, allowing different nucleotide specificities within the family.[1] The catalytic mechanism involves a nucleophilic attack by a glutamate (Glu222)-activated water molecule on the terminal phosphate, which is stabilized by the metal ion and adjacent backbone NH groups and side chains.[13] The catalytic site is fully conserved in NTPDase4 (Figure 3a), except Arg101, which corresponds to a histidine side chain in NTPDase1 and 2, or an arginine residue in microbial NTPDases. Most catalytic site residues are located on connecting loops from the central β sheets of domains I and II. Strikingly, in the current, open NTPDase4 conformation, the β sheets are displaced from each other such that half of the catalytic site is shifted by about 7 Å from its corresponding position in NTPDase-substrate complexes (Figure 3a). The metal ion is also absent. The protein likely transitions to a closed state upon substrate binding, or to allow substrate binding.

2.3 | Determinants of substrate specificity

The extracellular NTPDases 1, 2, 3, and 8 display broad specificity toward NTPs and NDPs, whereas the intracellular family members 4, 5, 6, and 7 exhibit more specific nucleotide preferences.[1] NTPDase4 hydrolyzes pyrimidines (UTP, UDP, CTP, and CDP) at higher rates than purines, and is almost inactive against ATP and ADP.[9,14] The nucleoside-binding region in these proteins consists of residues from domain II. Comparison of ATP analogue-bound NTPDase2[13] with apo NTPDase4 reveals differences in substrate-interacting residues that could

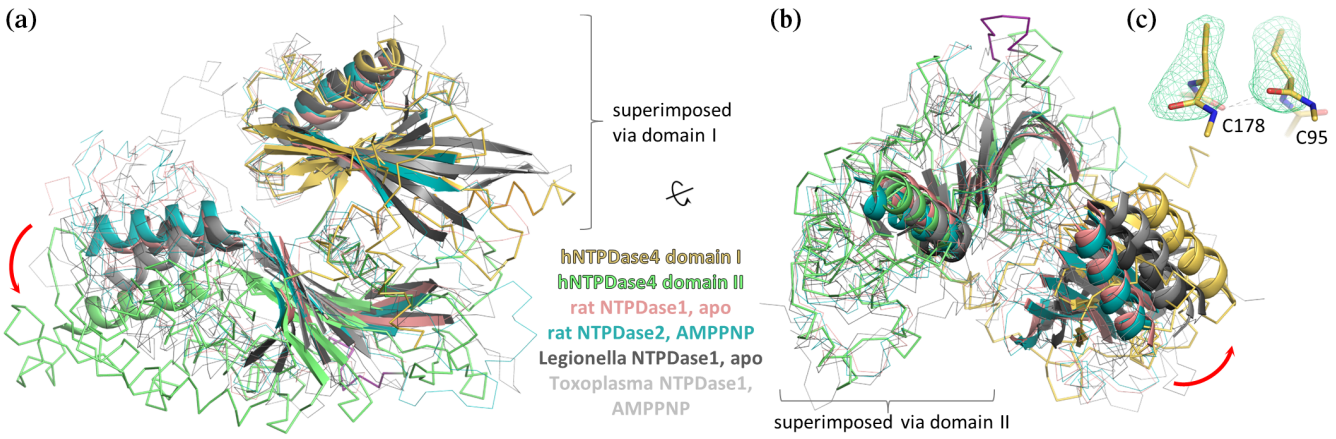

FIGURE 2 Domain orientation differences in NTPDases. (a) The crystal structures of human NTPDase4, rat NTPDase1 (PDB: 3ZX3),[10] rat NTPDase2 (PDB: 3CJA),[13] Legionella NTPDase1 in an open form (PDB: 4BR4)[11] and Toxoplasma NTPDase1 (PDB: 4KH4)[22] are superimposed via Domain I. The central β-sheets and two α-helices are shown as cartoons to illustrate the relative orientation differences, also represented by a red arrow. (b), As in a, with the structures superimposed via Domain II. The view is also rotated. (c) The simulated annealing F_o-F_c omit map of human NTPDase (C178 and C95 omitted) is contoured at 3σ

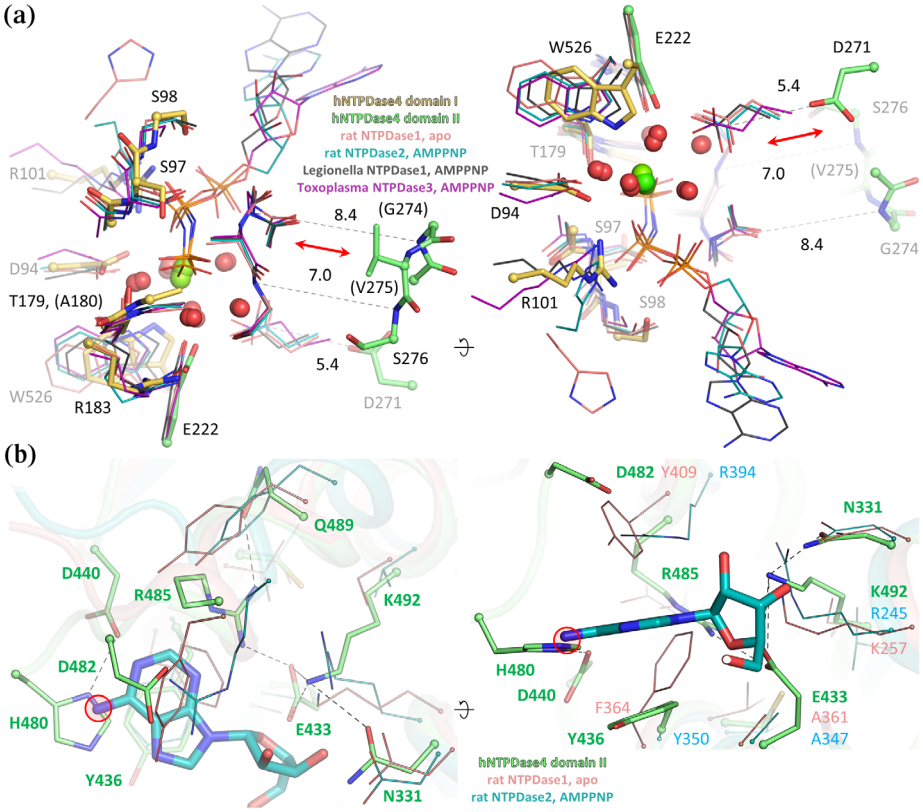

FIGURE 3 Active site and substrate-binding site of NTPDase4. (a) Comparison of human apo NTPDase4 active site residues with those of rat apo NTPDase1 (PDB: 3ZX3),[10] rat NTPDase2 with AMPPNP (PDB: 3CJA),[13] Legionella NTPDase1 with AMPPNP (PDB: 4BRA),[11] and Toxoplasma NTPDase3 with AMPPNP (PDB: 4A5A),[20] all superimposed via domain I. Human NTPDase4 residues are labeled, with backbone interactors in parentheses. The relative displacement of a loop from domain II is indicated by dashed lines (Å) and represented by a red arrow. Catalytically important water molecules (red spheres) and calcium or magnesium ions (green spheres) are shown. (b) Comparison of the putative nucleobase- and ribose-binding site of human apo NTPDase4 with that of rat apo NTPDase1 and rat NTPDase2 with AMPPNP, all superimposed via domain II. Polar contacts between side chains of human NTPDase4 (green) are indicated by dashed lines. A potential clash is represented by a red circle

explain the more restrictive specificity of the latter enzyme (Figure 3b). Asn331 and Lys492 are functionally conserved in the two proteins, as well as in NTPDase1,[10] and could form hydrogen bonds with the ribose moiety. Glu433 could also contact the ribose; this residue is replaced by alanine in NTPDase1 and 2. In the AMPPNP-NTPDase2 complex, the nucleobase is stacked between the side chains of a tyrosine and arginine residue, which correspond to phenylalanine and tyrosine residues in NTPDase1. Interestingly, although one of the two stacking interactions, Tyr436, is conserved in NTPDase4, the second residue that would form the opposite wall of this slot, Arg485, is instead oriented "inward," with its side chain stabilized by Glu433 and Gln489. These side chains could rearrange to enable cation-π stacking of Arg485 with the substrate. On the other hand, its current position would allow it to hydrogen-bond with the nucleobase. Two other NTPDase4-specific amino acids, Asp440 and His480, could also establish hydrogen bonds with the base. In their current orientation, however, His480 would clash with purines (A or G), but could accommodate the smaller pyrimidines such as U. All these differences could account for the narrower substrate selectivity of this enzyme relative to NTPDase1 and 2, which do not form specific hydrogen bonds with nucleobases.[11] These results remain to be experimentally verified, as other substrate orientations have also been observed within the NTPDase family.[11,22]

2.4 | NTPDase4 isoforms

Two isoforms of NTPDase4 have been reported: a long isoform (LALP70) found in lysosomal and autophagic vacuoles,[15] and a short isoform (LALP70v) missing a VSFASSQQ sequence in domain II (Figure 1a), found in the Golgi.[9] The long isoform is expressed at much higher levels in all tissues examined.[14] The variants also display somewhat different substrate specificities and dependency on metal ion concentration.[14,16] The crystal

structure of the long isoform is reported here (Figure 1b). The VSFASSQQ segment is located on the periphery on the protein, 25 Å away from the active site and 35 Å away from the nucleobase slot, and encompasses part of a helix and a loop (Figure 4a). Its sequence is highly conserved in vertebrates (Figure 4d). The corresponding loop is shorter in the other mammalian NTPDases (Figure 4b), except in NTPDase7 (Figure 4c), which is closest to NTPDase4 (65% identity). The crystal structure does not clarify the manner in which absence of this segment affects enzymatic properties, as it is unlikely to result in rearrangements that would reach the active site, based on the homolog structures. Its effect could be mediated indirectly through interdomain dynamics.

2.5 | NTPDase4 membrane interactions

The extracellular NTPDases 1, 2, 3, and 8, as well as NTPDase4 and 7, are anchored to lipid bilayers via two transmembrane helices, at the N- and C-terminus of the protein (Figure 1a). Disruption of the membrane attachment decreases NTPDase1 and 2 activity by 90% and affects their substrate preferences.[26] It is unknown whether these findings also apply to NTPDase4. The transmembrane helices may play a role in stabilizing or restricting interdomain motions, or enable oligomerization; these effects may be influenced by membrane lipid composition.[26] A notable feature found in domain II of the extracellular NTPDases is a potential membrane-

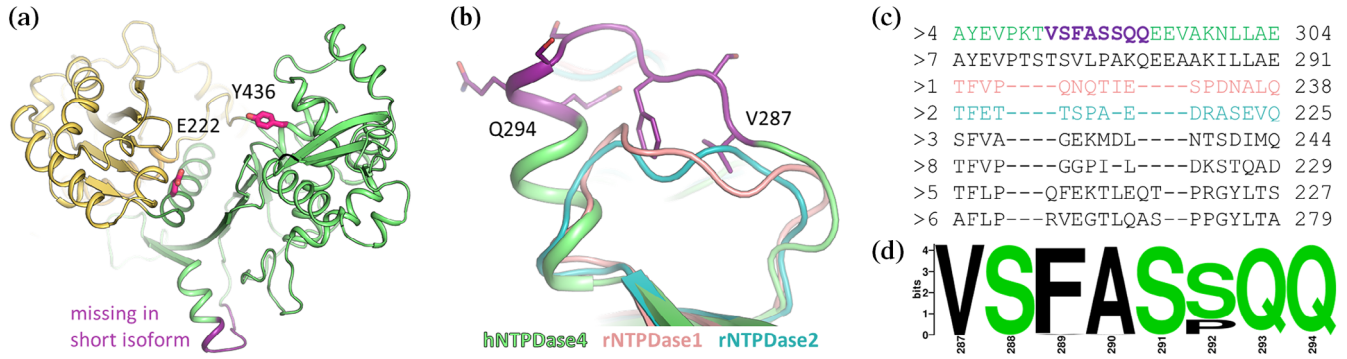

FIGURE 4 Isoforms of NTPDase4. (a) Location of the portion missing from the short isoform of human NTPDase4 (purple) relative to residues likely involved in substrate binding (Y436) and catalysis (E222, pink sticks). The crystal structure of the long isoform is shown. (b) This segment (residues 287–294) is compared with the corresponding loop in superimposed structures of rat NTPDase1 (PDB: 3ZX3)[10] and rat NTPDase2 (PDB: 3CJA).[13] (c) Structure-guided sequence alignment of this region in human NTPDases 1 through 8. Residue numbers correspond to the last residue shown in the alignment, for each NTPDase. (d) Sequence conservation in vertebrates of the NTPDase4 segment missing from the short isoform

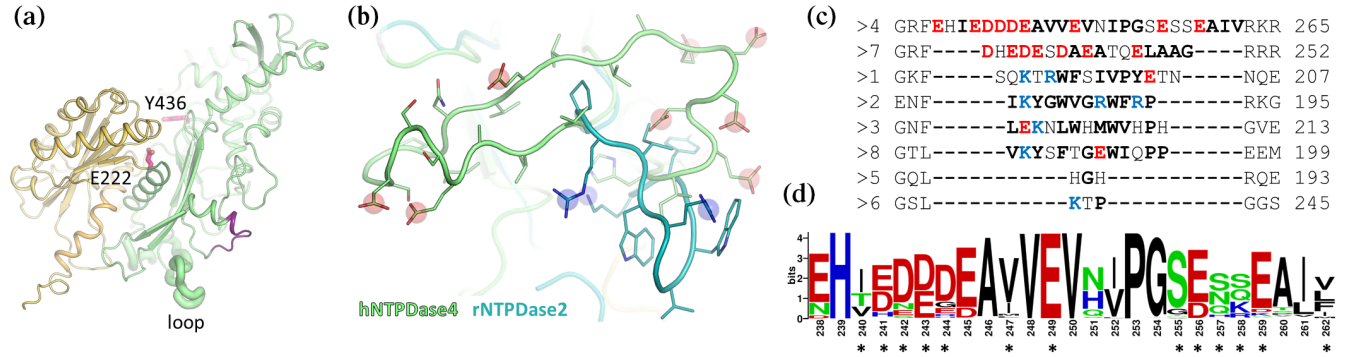

FIGURE 5 Putative membrane-interacting loop in NTPDases. (a) The human NTPDase4 loop corresponding to the potential membrane insertion segment of rat NTPDase2 (PDB: 3CJA)[13] is displayed as thick ribbon. Residues likely involved in substrate binding (Y436) and catalysis (E222) are shown as pink sticks. (b) Both enzymes are superimposed via domain II to illustrate conformational differences in this loop. Positively charged side chains are represented by blue spheres, and negatively charged ones, by red spheres. (c) Sequences alignment of the corresponding region of human NTPDases 1 through 8, with cationic residues in blue, anionic ones in red, and hydrophobic amino acids in bold. Residue numbers correspond to the last residue shown in the alignment, for each NTPDase. (d) Sequence conservation of the NTPDase4 loop in vertebrates. Side chains pointing away from the protein into the solvent are marked by asterisks

interacting loop containing hydrophobic and cationic residues.[10,13] The corresponding segment in NTPDase4 is located far from the active site, on the same side of the protein as the sites of membrane attachment at the ends of domain I (Figure 5a). Interestingly, this loop is longer and contains eight conserved, surface-exposed negatively charged residues instead of the cationic side chains of NTPDase2 (Figure 5b,d). It also lacks the bulky hydrophobic residues found in extracellular NTPDases (Figure 5c). Therefore, this loop is not expected to insert into the membrane in the case of NTPDase4 (and possibly NTPDase7).

The structural data presented here are a step toward understanding the function of the relatively poorly characterized enzyme NTPDase4. Further studies are needed to clarify its substrate selectivity and potential regulation at intracellular membranes.

3 | MATERIALS AND METHODS

3.1 | Protein expression and purification

Recombinant human NTPDase4 was expressed as a secreted protein in *Sf*9 insect cells infected with baculovirus. The construct started with the melittin signal peptide MKFLVNVALVFMVVYISYIYA followed by a hexahistidine tag DRHHHHHHKL and comprised the luminal portion of the enzyme (UniProt: Q9Y227, residues 58–559, long isoform containing the VSFASSQQ segment). The gene was cloned into a modified pFastBac vector downstream of a polyhedrin promoter and was transposed into a bacmid, which was transfected into *Sf*9 cells for baculovirus amplification. For expression, *Sf*9 cells were infected with 3.5% virus stock at 27°C for 64 hr. The protein was isolated from culture media by immobilized metal affinity chromatography (IMAC) with HisPur Ni-NTA resin (ThermoFisher Scientific). Bound proteins were washed in buffer (25 mM Tris–HCl pH 7.5, 500 mM NaCl, 10 mM imidazole) and eluted with the same buffer containing 250 mM imidazole. The eluate was concentrated to 0.5 ml, loaded on a Superdex 200 Increase size exclusion chromatography (SEC) column (GE Healthcare Life Sciences) in buffer (10 mM Tris–HCl pH 7.5, 100 mM NaCl), and concentrated to 5–10 mg/ml.

3.2 | X-ray crystallography

Human NTPDase4 crystallized in 0.2 M potassium-sodium tartrate with 20% PEG 3350. Crystals were grown by sitting drop vapor diffusion at 22°C and were flash-frozen after brief soaking in well solution supplemented with 20% glycerol. X-ray diffraction data were collected at 100 K on beamline 08ID-1 at the Canadian Macromolecular

TABLE 1 Crystallographic data collection and structure refinement statistics

	Human NTPDase4
PDB code	6WG5
Data collection	
Space group	P 2_1 2_1 2_1
Unit cell a, b, c (Å)	56.4, 101.8, 129.6
Unit cell α, β, γ (°)	90, 90, 90
X-ray wavelength (Å)	0.98
Resolution range (Å)	50–2.60 (2.69–2.60)
Total reflections	171,188 (15,531)
Unique reflections	23,613 (2,318)
Multiplicity	7.2 (6.7)
Completeness (%)	100 (100)
R_{meas} (%)	10.8 (159.7)
Mean I/σ(I)	18.5 (1.5)
$CC_{1/2}$	1.00 (0.62)
Wilson B factor (Å^2)	41.3
Refinement	
Protein copies per ASU	1
Resolution range (Å)	49.30–2.60 (2.69–2.60)
Anisotropic limits a, b, c (Å)	2.69, 2.61, 2.65
Completeness (%)	95 (67)
Reflections used	22,484 (1,571)
Reflections for R_{free}	1,864 (130)
R_{work} (%)	17.8 (24.0)
R_{free} (%)	21.6 (27.9)
RMSD bond lengths (Å)	0.002
RMSD bond angles (°)	0.51
Ramachandran favored (%)	97.6
Ramachandran allowed (%)	2.2
Ramachandran outliers (%)	0.2
Rotamer outliers (%)	0.7
Clashscore	0.76
Average B factor (Å^2)	52.0 (4,228)
Protein	52.2 (3,996)
Glycans	77.2 (28)
Water	45.3 (204)

Note: Values in parentheses are for the highest resolution shell, except for the "Average B factor" section, where they specify the number of nonhydrogen atoms. Anisotropic limits are the approximate resolution to which data extends along the three cell axes after ellipsoidal truncation in postprocessing.

Abbreviations: ASU, asymmetric unit. RMSD, root mean square deviation.

Crystallography Facility (CMCF), Canadian Light Source (CLS) with a Rayonix MX300 CCD detector.

3.3 | Structure determination

Data were processed by HKL2000[27] with auto-corrections enabled. This option applies corrective procedures including ellipsoidal truncation, which reduces high-resolution data completeness based on anisotropy. This is made apparent in the number of reflections and completeness values in "Data collection" versus "Refinement" in Table 1. The structure was solved by molecular replacement with the rat NTPDase1 structure split into two domains (PDB: 3ZX3)[10] by Phaser[28] in Phenix[29] and manually built in Coot.[30] Refinement was carried out by phenix.refine[31] with translation–libration–screw (TLS) parameters applied. Crystallographic data collection and structure refinement statistics are presented in Table 1. Structural images were prepared with PyMOL (The PyMOL Molecular Graphics System, Version 1.3 Schrödinger, LLC).

3.4 | Enzymatic activity assay

Purified NTPD4 (crystallized construct) was incubated at 2 nM in 50 mM Tris–HCl pH 7.5 with 100 mM NaCl and 5 mM $CaCl_2$ in presence of UDP for 1 hr at 37°C. Four volumes of BIOMOL Green phosphate detection reagent (Enzo Life Sciences, Farmingdale, NY) were then added, followed by incubation for 20 min and absorbance measurement at 620 nm. Substrate hydrolysis was quantified with a phosphate standard curve.

ACKNOWLEDGMENTS

Part or all of the research described in this article was performed using beamline 08ID-1 at the Canadian Light Source, a national research facility of the University of Saskatchewan, which is supported by the Canada Foundation for Innovation (CFI), the Natural Sciences and Engineering Research Council (NSERC), the National Research Council (NRC), the Canadian Institutes of Health Research (CIHR), the Government of Saskatchewan, and the University of Saskatchewan. Bhushan Nagar is supported by a grant from the Canadian Institutes of Health Research (CIHR grant MOP-133535).

AUTHOR CONTRIBUTIONS

Alexei Gorelik: Conceptualization; data curation; formal analysis; investigation; methodology; writing-original draft; writing-review and editing. **Jonathan Labriola:** Conceptualization; data curation; formal analysis; investigation; methodology; writing-review and editing. **Katalin Illes:** Investigation; methodology; writing-review and editing. **Bhushan Nagar:** Funding acquisition; project administration; supervision; writing-review and editing.

CONFLICT OF INTEREST

The authors declare no conflicting interests.

DATA AVAILABILITY STATEMENT

Atomic coordinates and structure factors were deposited into the Protein Data Bank under the accession code 6WG5.

ORCID

Alexei Gorelik https://orcid.org/0000-0001-6236-4633

REFERENCES

1. Zimmermann H, Zebisch M, Strater N. Cellular function and molecular structure of ecto-nucleotidases. Purinergic Signal. 2012;8:437–502.
2. Knowles AF. The gda1_cd39 superfamily: Ntpdases with diverse functions. Purinergic Signal. 2011;7:21–45.
3. al-Rashida M, Iqbal J. Therapeutic potentials of ecto-nucleoside triphosphate diphosphohydrolase, ecto-nucleotide pyrophosphatase/phosphodiesterase, ecto-5′-nucleotidase, and alkaline phosphatase inhibitors. Med Res Rev. 2014;34:703–743.
4. Giuliani AL, Sarti AC, Di Virgilio F. Extracellular nucleotides and nucleosides as signalling molecules. Immunol Lett. 2019;205:16–24.
5. Hirschberg CB, Robbins PW, Abeijon C. Transporters of nucleotide sugars, atp, and nucleotide sulfate in the endoplasmic reticulum and golgi apparatus. Annu Rev Biochem. 1998;67:49–69.
6. Fang M, Shen Z, Huang S, et al. The er udpase entpd5 promotes protein n-glycosylation, the warburg effect, and proliferation in the pten pathway. Cell. 2010;143:711–724.
7. Braun N, Fengler S, Ebeling C, Servos J, Zimmermann H. Sequencing, functional expression and characterization of rat ntpdase6, a nucleoside diphosphatase and novel member of the ecto-nucleoside triphosphate diphosphohydrolase family. Biochem J. 2000;351:639–647.
8. Knowles AF. The single ntpase gene of *Drosophila melanogaster* encodes an intracellular nucleoside triphosphate diphosphohydrolase 6 (ntpdase6). Arch Biochem Biophys. 2009;484:70–79.
9. Wang TF, Guidotti G. Golgi localization and functional expression of human uridine diphosphatase. J Biol Chem. 1998;273:11392–11399.
10. Zebisch M, Krauss M, Schafer P, Strater N. Crystallographic evidence for a domain motion in rat nucleoside triphosphate diphosphohydrolase (ntpdase) 1. J Mol Biol. 2012;415:288–306.
11. Zebisch M, Krauss M, Schafer P, Lauble P, Strater N. Crystallographic snapshots along the reaction pathway of nucleoside triphosphate diphosphohydrolases. Structure. 2013;21:1460–1475.
12. Zebisch M, Baqi Y, Schafer P, Muller CE, Strater N. Crystal structure of ntpdase2 in complex with the sulfoanthraquinone inhibitor psb-071. J Struct Biol. 2014;185:336–341.

13. Zebisch M, Strater N. Structural insight into signal conversion and inactivation by ntpdase2 in purinergic signaling. Proc Natl Acad Sci U S A. 2008;105:6882–6887.
14. Biederbick A, Kosan C, Kunz J, Elsasser HP. First apyrase splice variants have different enzymatic properties. J Biol Chem. 2000;275:19018–19024.
15. Biederbick A, Rose S, Elsasser HP. A human intracellular apyrase-like protein, lalp70, localizes to lysosomal/autophagic vacuoles. J Cell Sci. 1999;112:2473–2484.
16. Biederbick A, Rosser R, Storre J, Elsasser HP. The vsfassqq motif confers calcium sensitivity to the intracellular apyrase lalp70. BMC Biochem. 2004;5:8.
17. Zhang Z, Wu H, Chen Z, Li G, Liu B. Circular rna atxn7 promotes the development of gastric cancer through sponging mir-4319 and regulating entpd4. Cancer Cell Int. 2020; 20:25.
18. Bork P, Sander C, Valencia A. An atpase domain common to prokaryotic cell cycle proteins, sugar kinases, actin, and hsp70 heat shock proteins. Proc Natl Acad Sci U S A. 1992;89: 7290–7294.
19. Summers EL, Cumming MH, Oulavallickal T, Roberts NJ, Arcus VL. Structures and kinetics for plant nucleoside triphosphate diphosphohydrolases support a domain motion catalytic mechanism. Protein Sci. 2017;26:1627–1638.
20. Krug U, Zebisch M, Krauss M, Strater N. Structural insight into activation mechanism of toxoplasma gondii nucleoside triphosphate diphosphohydrolases by disulfide reduction. J Biol Chem. 2012;287:3051–3066.
21. Krug U, Totzauer R, Strater N. The crystal structure of toxoplasma gondii nucleoside triphosphate diphosphohydrolase 1 represents a conformational intermediate in the reductive activation mechanism of the tetrameric enzyme. Proteins. 2013;81:1271–1276.
22. Krug U, Totzauer R, Zebisch M, Strater N. The atp/adp substrate specificity switch between toxoplasma gondii ntpdase1 and ntpdase3 is caused by an altered mode of binding of the substrate base. Chembiochem. 2013;14:2292–2300.
23. Matoba K, Shiba T, Takeuchi T, et al. Crystallization and preliminary x-ray structural analysis of nucleoside triphosphate hydrolases from neospora caninum and toxoplasma gondii. Acta Crystallogr. 2010;F66:1445–1448.
24. Vivian JP, Riedmaier P, Ge H, et al. Crystal structure of a legionella pneumophila ecto -triphosphate diphosphohydrolase, a structural and functional homolog of the eukaryotic ntpdases. Structure. 2010;18:228–238.
25. Zebisch M, Krauss M, Schafer P, Strater N. Structures of legionella pneumophila ntpdase1 in complex with polyoxometallates. Acta Cryst. 2014;D70:1147–1154.
26. Grinthal A, Guidotti G. Cd39, ntpdase 1, is attached to the plasma membrane by two transmembrane domains. Why? Purinergic Signal. 2006;2:391–398.
27. Otwinowski Z, Minor W. Processing of x-ray diffraction data collected in oscillation mode. Methods Enzymol. 1997;276: 307–326.
28. McCoy AJ, Grosse-Kunstleve RW, Adams PD, Winn MD, Storoni LC, Read RJ. Phaser crystallographic software. J Appl Cryst. 2007;40:658–674.
29. Adams PD, Afonine PV, Bunkoczi G, et al. Phenix: A comprehensive python-based system for macromolecular structure solution. Acta Cryst D. 2010;66:213–221.
30. Emsley P, Lohkamp B, Scott WG, Cowtan K. Features and development of coot. Acta Cryst D. 2010;66:486–501.
31. Afonine PV, Grosse-Kunstleve RW, Echols N, et al. Towards automated crystallographic structure refinement with phenix. Refine. Acta Crystallogr. 2012;D68:352–367.

How to cite this article: Gorelik A, Labriola JM, Illes K, Nagar B. Crystal structure of the nucleotide-metabolizing enzyme NTPDase4. *Protein Science*. 2020;29:2054–2061. https://doi.org/10.1002/pro.3926